

STRUCTURAL PHASE TRANSITION INDUCED BY PRESSURE IN THE ORDERED ALLOY FeRh

M. RAJAGOPALAN

Max Planck Institute fur Festkorperforschung, D-70589 Stuttgart, Germany
Department of Physics, Anna University, Chennai-600025, India
mraja1948@yahoo.co.in

Received 4 November 2004

First-principles density functional calculation of the total energy as a function of volume has been performed by the TB-LMTO approach for the ordered alloy FeRh in the anti-ferromagnetic state. We find that FeRh undergoes a structural phase transition from NaCl-type to tetragonal-type structure around 20.3 GPa which is in best agreement with the recent experimental observation. The calculations show that the energy of the antiferromagnetic ground state is lower than the one for the ferromagnetic state at ambient conditions.

Keywords: Electronic structure; anti-ferromagnetic state; structural phase transition; density of states; TB-LMTO method.

1. Introduction

From the experimental and theoretical points of view, the ordered compound FeRh is of great interest due to the fact that it exhibits three different magnetic phases in quick succession as the temperature increases without any appreciable change in the crystal structure. This ordered alloy, with base centered cubic CsCl-type structure was found to undergo a first order phase transition from an anti-ferromagnetic state (AFM) to a ferromagnetic state (FM) state at a temperature of 360 K.^{1,2} This transition was accompanied by an abrupt increase in lattice constant,³ an increase of iron magnetic moment,⁴ a large increase in entropy⁵ and a fall in electrical resistivity.⁶ Another transition from the FM state to the paramagnetic (PM) state was reported around 650 K.⁶ The transition temperatures are very sensitive to small changes in the concentration. Because of the above mentioned properties, FeRh alloys are considered a potential material for various kinds of sensors. The crystal structure of this compound in its three magnetic phases has been determined by X-ray and neutron measurements.⁷ Since then many experimental studies of AFM to FM transitions have been made, exhibiting its sensitivity to experimental conditions such as pressure,⁸ presence of impurities and deviations from stoichiometry.⁹ In addition, the magnetic moments have been measured by many authors.^{4,9} For the

compound in the FM state, the magnetic moments are $2.84 \mu_B$ and $0.8 \mu_B$ on the iron and rhodium sites, respectively. In the AFM state, the moment on the iron site is $3.3 \mu_B$ and almost zero on the rhodium site.¹⁰

The self consistent band structure of paramagnetic, ferromagnetic and anti-ferromagnetic ordered FeRh are calculated using the linear muffin tin method by Koenig.¹¹ Moruzzi and Marcus¹² had performed the band structure calculation based on the augmented spherical wave method and their calculations reveal the co-existence of the AFM and FM states over a wide range of volume but the zero pressure equilibrium state was found to be that of the AFM one. Recently, the equi-atomic alloy FeRh was studied by Kuncser *et al.*¹³ by a high pressure energy dispersive X-ray diffraction experiment and they had reported a structural phase transition around 19 GPa. The motivation of the present work emerged from the experimental work summarized above. In particular, I studied the pressure induced phase transition by performing the electronic structure and total energy calculation by means of the tight binding linear muffin tin orbital method (TB-LMTO) within the density functional formalism. The rest of the paper is organized as follows. The computational details are given in Sec. 2. The results are summarized and discussed in the last section.

2. Methodology of Calculation

In the FM state, the lattice is of CsCl-type. The positions of caesium and rhodium atoms are $(0, 0, 0)$ and $(0.5, 0.5, 0.5)$ respectively in the simple cubic cell. In the AFM state the lattice can be considered as face centered cubic and the positions of the four atoms in the cell are $(0, 0, 0)$ and $(0.5, 0.5, 0.5)$ for the iron atoms and $(0.25, 0.25, 0.25)$ and $(-0.25, -0.25, -0.25)$ for the rhodium atoms. We had performed the band structure calculations in the FM state first. Within the density functional formalism, the electronic structure calculations was performed using the TB-LMTO approach.^{14,15} The exchange-correlation potential within the local density approximation was calculated using the parametrization scheme of von Barth and Hedin.¹⁶ The scalar relativistic approach, which includes the mass velocity and Darwin corrections but omits the spin orbit coupling, is included in the present study. The tetrahedron method¹⁷ was used to perform all k space integration. The sphere radii were chosen in such a way that the maximum overlap between any two spheres is approximately 15%.

3. Results and Discussion

The electronic structure and the total energies of FeRh in the FM state are obtained by performing the spin polarized band structure calculation as a function of cell volume. The total energies are fitted to the equation of state¹⁸ and the pressure volume relation is obtained. The equilibrium lattice parameters and the bulk modulus are also obtained. The magnetic moment at the iron site ($3.08 \mu_B$) and at

rhodium site ($1.02 \mu_B$) compares well with the values.¹² As expected, the magnetic moment decreases as the pressure increases.

The calculations are repeated for the AFM state by performing the spin polarized calculation as a function of cell volume in the NaCl-type structure. The total energies are fitted to the equation of state and the ground state properties are obtained. The calculated bulk modulus is 2.53 MBar. From the total energy calculations, we find that the difference in energy between the AFM and FM state is around 9 mRyd. Also, the AFM state is more stable than the FM state. In the AFM state, the local magnetic moment is $2.93 \mu_B$ at the iron site and almost zero at the rhodium site which is in agreement with the earlier calculation.¹² With increase of pressure, there is a decrease in the magnetic moment.

In order to look for a possible structural phase transition, the calculations are performed in the tetragonal structure with space group number 124. The unit cell is doubled along the c -axis. The iron atoms are positioned at $(0, 0, 0)$ and $(0, 0, 0.5)$ and the rhodium atoms at $(0.5, 0.5, 0.25)$ and $(0.5, 0.5, -0.25)$. The electronic structure and the total energies are obtained as a function of cell volume by performing spin polarized calculations. The total energies are fitted to the equation of state. In Fig. 1 we present the total energies of FeRh as a function of V/V_0 in the three different structures, namely, FM in the CsCl-type, AFM in the NaCl-type and AFM in the tetragonal-type structure. In order to determine the transition pressure, the Gibbs free energy is calculated for the two phases using the relation

$$G = E_{\text{TOT}} + PV - TS. \quad (1)$$

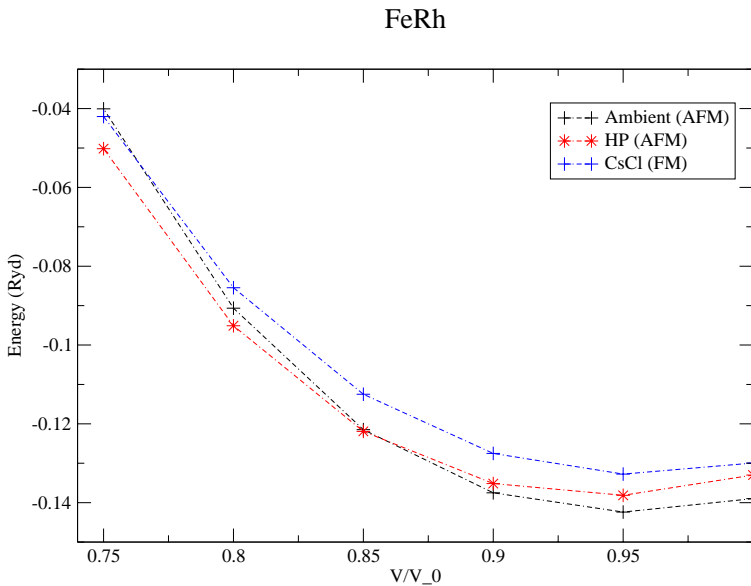


Fig. 1. Total energy versus V/V_0 curves.

Since the calculations are done at 0 K, the Gibbs free energy is equal to enthalpy. The transition pressure is obtained as the pressure at which the enthalpies of the two phases are equal. From this study, we find the transition pressure to be 20.3 GPa which compares well with the recent experimental observation.¹³

The band structure and the density of states are plotted for the two different structures for the AFM state and are given in Figs. 2–5. The band profile of FeRh

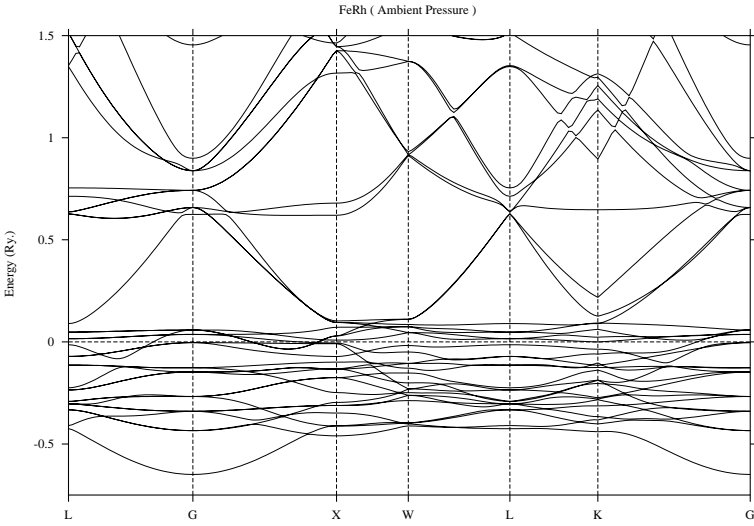


Fig. 2. Band structure of FeRh at ambient pressure in NaCl structure type.

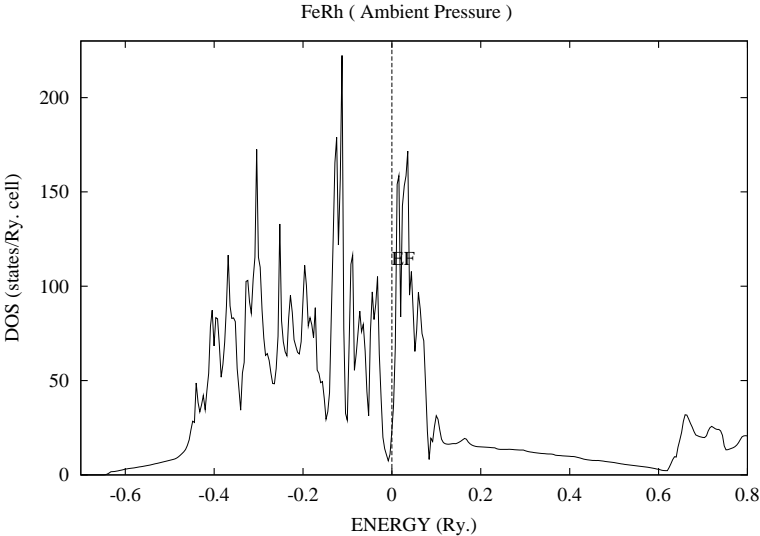


Fig. 3. Density of states of FeRh in NaCl structure.

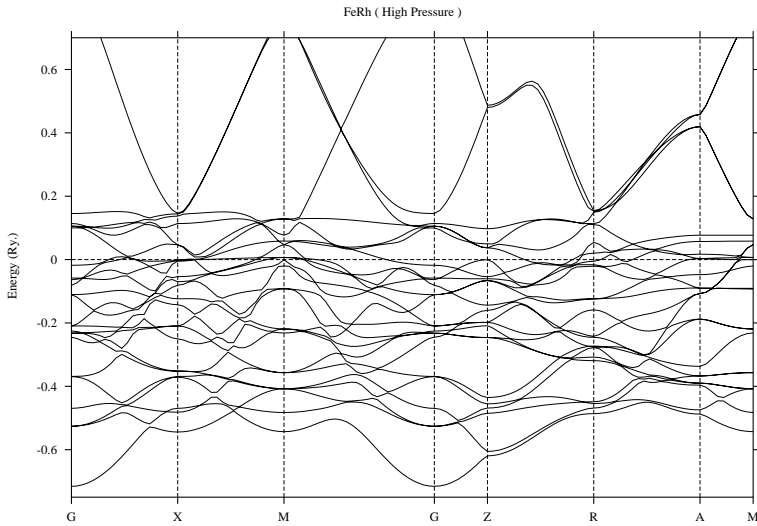


Fig. 4. Band structure of FeRh in the tetragonal structure.

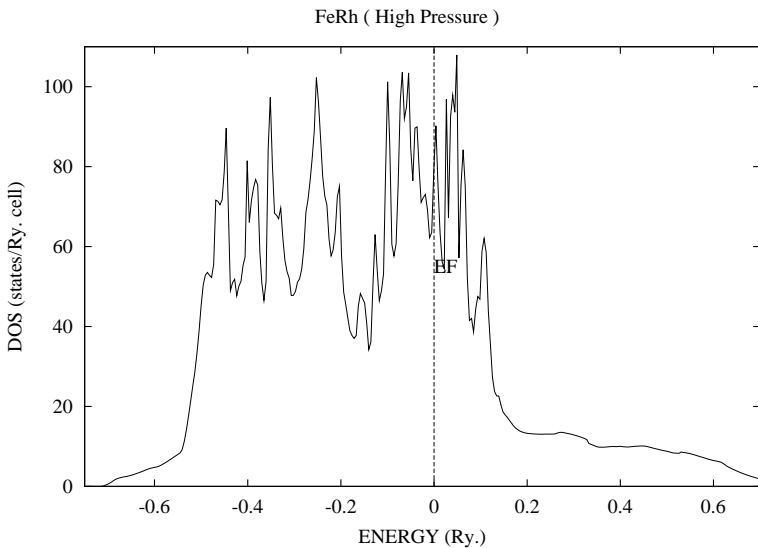


Fig. 5. Density of states of FeRh in the tetragonal structure.

in the NaCl structure type is in good agreement with those obtained by Koenig.¹¹ The lowest lying band is due to Rh “*s*-like” states followed by Fe “*s*-like” states. Above these bands lie the Rh “*d*-like” and Fe “*d*-like” states. The “*p*-like” states of Fe and Rh are above the Fermi level. The density of states at the Fermi level and the partial number of electrons are also calculated as a function of cell volume and presented in Table 1 along with the other parameters. From the table, one observes

Table 1. Partial number of electrons and total density of states in NaCl structure.

V/V_0	Partial number of electrons				Partial number of electrons			DOS (States/ Ryd-cell)
	Fe				Rh			
	<i>s</i>	<i>p</i>	<i>d</i>		<i>s</i>	<i>p</i>	<i>d</i>	
0.95	0.299	0.357	1.747	(up)	0.324	0.399	3.842	11.80
	0.314	0.372	4.644	(dn)	0.324	0.399	3.842	
0.90	0.296	0.360	1.809	(up)	0.323	0.404	3.824	12.69
	0.310	0.374	4.599	(dn)	0.323	0.404	3.824	
0.85	0.294	0.364	1.888	(up)	0.321	0.408	3.805	14.40
	0.305	0.376	4.542	(dn)	0.321	0.408	3.805	
0.80	0.291	0.366	1.994	(up)	0.319	0.411	3.785	21.24
	0.299	0.378	4.466	(dn)	0.319	0.411	3.785	
0.75	0.288	0.367	2.134	(up)	0.317	0.413	3.762	35.00
	0.293	0.377	4.364	(dn)	0.317	0.413	3.762	

Table 2. Partial number of electrons and total density of states in tetragonal structure.

V/V_0	Partial number of electrons				Partial number of electrons			DOS (States/ Ryd-cell)
	Fe				Rh			
	<i>s</i>	<i>p</i>	<i>d</i>		<i>s</i>	<i>p</i>	<i>d</i>	
1.00	0.292	0.342	1.660	(up)	0.332	0.396	3.878	37.721
	0.317	0.348	4.694	(dn)	0.332	0.396	3.878	
0.95	0.289	0.346	1.714	(up)	0.331	0.403	3.859	36.737
	0.312	0.352	4.655	(dn)	0.331	0.403	3.859	
0.90	0.287	0.349	1.782	(up)	0.330	0.409	3.840	35.863
	0.308	0.354	4.607	(dn)	0.330	0.409	3.840	
0.85	0.284	0.351	1.879	(up)	0.329	0.413	3.820	40.121
	0.303	0.358	4.536	(dn)	0.329	0.413	3.820	
0.80	0.281	0.330	2.041	(up)	0.327	0.416	3.799	40.858
	0.296	0.355	4.414	(dn)	0.327	0.416	3.799	
0.75	0.277	0.351	2.200	(up)	0.325	0.419	3.776	38.734
	0.290	0.355	4.292	(dn)	0.325	0.419	3.776	

that there is an increase in the density of states as the pressure increases. But the increment in the value of the density of states is less up to a compression of $0.85 V_0$ and then there is a sudden increase at $0.80 V_0$. From the same table, it can also be seen that the number of “*d*-like” electrons at the Fe site increases slowly for the up spin up to $0.85 V_0$ and then there is a jump around $0.80 V_0$. The band structure of FeRh along the high symmetry directions in the high pressure phase, namely, tetragonal, is given in Fig. 4. Also, in this phase, the band structure has similar features as that of the ambient phase. The bands which are close to the Fermi level are due to the Rh “*d*” and Fe “*d*-like” states. The density of states at the Fermi level is also calculated and given in Fig. 5. The density of states first decreases as the pressure increases and then there is a sudden jump at $0.85 V_0$ and then it starts decreasing (see Table 2). This sudden jump in the density of states occurs

at a pressure of 20.3 GPa at which FeRh undergoes a structural phase transition from the NaCl-type to the tetragonal-type structure in the AFM state which is in agreement with the recent experimental observation.¹³

In summary, we have performed the spin polarized band structure and total energy calculation in the AFM state of FeRh in two different structures namely the NaCl and tetragonal types. From the present study we find that FeRh undergoes a structural phase transition around 20.3 GPa which is in good agreement with the recent experimental observation.¹³ We also observed that the magnetic moment at the Fe site decreases as the pressure increases and the local magnetic moment at the Rh site is almost zero.

Acknowledgment

The author thanks Max Planck Society and Prof. O. K. Andersen for the hospitality rendered and M. Alouani for useful discussions.

References

1. V. L. Maruzzi and P. M. Marcus, *Phys. Rev.* **B46**, 2864 (1992).
2. M. R. Ibarra and P. A. Algarabel, *Phys. Rev.* **B50**, 4196 (1994).
3. F. Bergevin and M. Muldrew, *C. R. Acad. Sci.* **252**, 1347 (1961).
4. G. Shirane, C. W. Chen, F. A. Flinn and R. Nathans, *Phys. Rev.* **131**, 183 (1963).
5. J. S. Konvel, *J. Appl. Phys.* **37**, 1257 (1966).
6. J. S. Konvel and C. C. Hartelins, *J. Appl. Phys.* **33**, 1343 (1962).
7. F. Bertaut, F. Bergevin and G. Roullet, *C. R. Acad. Sci.* **256**, 1688 (1962).
8. L. I. Vinokurova, A. V. Vlasov and M. Pardavi-Horvath, *Physica Stat. Solid* **B78**, 353 (1976).
9. G. Shirane, R. Nathans and C. W. Chen, *Phys. Rev.* **A134**, 1547 (1964).
10. C. S. Hartigai, *Phys. Lett.* **17**, 178 (1965).
11. C. Koenig, *J. Phys.* **F12**, 1123 (1982).
12. V. L. Moruzzi and P. M. Marcus, *Phys. Rev.* **B48**, 16106 (1993).
13. V. Kuncser, R. Nicula, U. Ponkratz, A. Jianu, M. Stir, E. Burkl and G. Filoti, *J. Alloys Compds.* **386**, 28 (2005).
14. O. K. Andersen, *Phys. Rev.* **B12**, 3060 (1975).
15. O. K. Andersen and O. Jepsen, *Phys. Rev Lett.* **53**, 2571 (1984).
16. U. von Barth and L. Hedin, *J. Phys.* **C5**, 1629 (1972).
17. O. Jepsen and O. K. Andersen, *Solid State Commun.* **9**, 1763 (1971).
18. F. Birch, *J. Geophys. Res.* **83**, 1257 (1978).